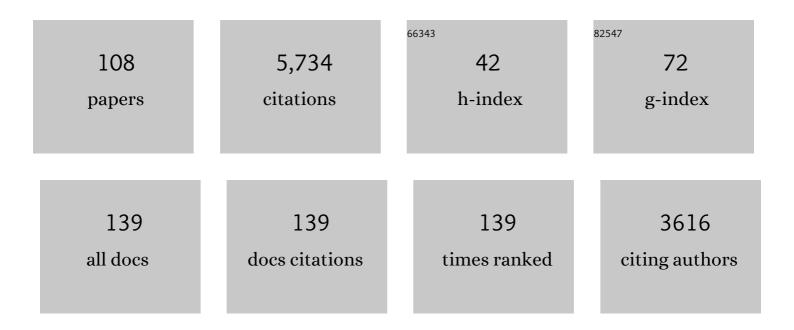
## Eleonore Stutzmann

List of Publications by Year in descending order

Source: https://exaly.com/author-pdf/4477919/publications.pdf Version: 2024-02-01



#	Article	IF	CITATIONS
1	Initial results from the InSight mission on Mars. Nature Geoscience, 2020, 13, 183-189.	12.9	274
2	Ocean wave sources of seismic noise. Journal of Geophysical Research, 2011, 116, .	3.3	246
3	SEIS: Insight's Seismic Experiment for Internal Structure of Mars. Space Science Reviews, 2019, 215, 12.	8.1	238
4	Constraints on the shallow elastic and anelastic structure of Mars from InSight seismic data. Nature Geoscience, 2020, 13, 213-220.	12.9	207
5	Using instantaneous phase coherence for signal extraction from ambient noise data at a local to a global scale. Geophysical Journal International, 2011, 184, 494-506.	2.4	194
6	The seismicity of Mars. Nature Geoscience, 2020, 13, 205-212.	12.9	194
7	How ocean waves rock the Earth: Two mechanisms explain microseisms with periods 3 to 300 s. Geophysical Research Letters, 2015, 42, 765-772.	4.0	188
8	Seismic detection of the martian core. Science, 2021, 373, 443-448.	12.6	169
9	Infragravity waves: From driving mechanisms to impacts. Earth-Science Reviews, 2018, 177, 774-799.	9.1	165
10	Thickness and structure of the martian crust from InSight seismic data. Science, 2021, 373, 438-443.	12.6	140
11	Convective patterns under the Indo-Atlantic « box ». Earth and Planetary Science Letters, 2005, 239, 233-252.	4.4	138
12	GEOSCOPE Station Noise Levels. Bulletin of the Seismological Society of America, 2000, 90, 690-701.	2.3	131
13	Anisotropic structure of the African upper mantle from Rayleigh and Love wave tomography. Physics of the Earth and Planetary Interiors, 2006, 155, 48-62.	1.9	125
14	Global climate imprint on seismic noise. Geochemistry, Geophysics, Geosystems, 2009, 10, .	2.5	112
15	Numerical modeling of the Mount Steller landslide flow history and of the generated long period seismic waves. Geophysical Research Letters, 2012, 39, .	4.0	108
16	Modelling long-term seismic noise in various environments. Geophysical Journal International, 2012, 191, 707-722.	2.4	104
17	Buckling instabilities of subducted lithosphere beneath the transition zone. Earth and Planetary Science Letters, 2007, 254, 173-179.	4.4	97
18	Polarized Farth's ambient microseismic noise. Geochemistry, Geophysics, Geosystems, 2011, 12, n/a-n/a,	2.5	88

#	Article	IF	CITATIONS
19	Atmospheric Science with InSight. Space Science Reviews, 2018, 214, 1.	8.1	88
20	Modelling secondary microseismic noise by normal mode summation. Geophysical Journal International, 2013, 193, 1732-1745.	2.4	86
21	Mantle plumes: Thin, fat, successful, or failing? Constraints to explain hot spot volcanism through time and space. Geophysical Research Letters, 2008, 35, .	4.0	83
22	Imaging the lithospheric structure beneath the Indian continent. Journal of Geophysical Research: Solid Earth, 2016, 121, 7450-7468.	3.4	78
23	Understanding seismic heterogeneities in the lower mantle beneath the Americas from seismic tomography and plate tectonic history. Journal of Geophysical Research, 2007, 112, .	3.3	77
24	Detection, Analysis, and Removal of Glitches From InSight's Seismic Data From Mars. Earth and Space Science, 2020, 7, e2020EA001317.	2.6	75
25	Modelling the ocean site effect on seismic noise body waves. Geophysical Journal International, 2014, 197, 1096-1106.	2.4	74
26	Numerical modeling of the Mount Meager landslide constrained by its force history derived from seismic data. Journal of Geophysical Research: Solid Earth, 2015, 120, 2579-2599.	3.4	71
27	Global tomography using seismic hum. Geophysical Journal International, 2016, 204, 1222-1236.	2.4	70
28	Companion guide to the marsquake catalog from InSight, Sols 0–478: Data content and non-seismic events. Physics of the Earth and Planetary Interiors, 2021, 310, 106597.	1.9	64
29	Azores hotspot signature in the upper mantle. Journal of Volcanology and Geothermal Research, 2006, 156, 23-34.	2.1	62
30	From seismic noise to ocean wave parameters: General methods and validation. Journal of Geophysical Research, 2012, 117, .	3.3	62
31	An inverse technique for retrieving higher mode phase velocity and mantle structure. Geophysical Journal International, 1993, 113, 669-683.	2.4	61
32	Phenomenal Sea States and Swell from a North Atlantic Storm in February 2011: A Comprehensive Analysis. Bulletin of the American Meteorological Society, 2012, 93, 1825-1832.	3.3	60
33	The French Pilot Experiment OFM-SISMOBS: first scientific results on noise level and event detection. Physics of the Earth and Planetary Interiors, 1994, 84, 321-336.	1.9	58
34	How moderate sea states can generate loud seismic noise in the deep ocean. Geophysical Research Letters, 2012, 39, .	4.0	57
35	On the shaping factors of the secondary microseismic wavefield. Journal of Geophysical Research: Solid Earth, 2015, 120, 6241-6262.	3.4	53
36	Observations of the seasonality of the Antarctic microseismic signal, and its association to sea ice variability. Geophysical Research Letters, 2011, 38, n/a-n/a.	4.0	52

ELEONORE STUTZMANN

#	Article	IF	CITATIONS
37	Anisotropic tomography of the Atlantic Ocean. Physics of the Earth and Planetary Interiors, 2002, 132, 237-248.	1.9	51
38	Upper mantle structure of shear-waves velocities and stratification of anisotropy in the Afar Hotspot region. Tectonophysics, 2008, 462, 164-177.	2.2	51
39	Stratification of the Earth beneath the Azores from P and S receiver functions. Earth and Planetary Science Letters, 2010, 299, 91-103.	4.4	51
40	Tracking major storms from microseismic and hydroacoustic observations on the seafloor. Geophysical Research Letters, 2014, 41, 8825-8831.	4.0	45
41	Mantle upwellings and convective instabilities revealed by seismic tomography and helium isotope geochemistry beneath eastern Africa. Geophysical Research Letters, 2007, 34, .	4.0	44
42	Cape Verde hotspot from the upper crust to the top of the lower mantle. Earth and Planetary Science Letters, 2012, 319-320, 259-268.	4.4	44
43	Ray-theoretical modeling of secondary microseism <i>P</i> waves. Geophysical Journal International, 2016, 206, 1730-1739.	2.4	44
44	Extracting surface waves, hum and normal modes: time-scale phase-weighted stack and beyond. Geophysical Journal International, 2017, 211, 30-44.	2.4	44
45	Detection of microseismic compressional ( <i>P</i> ) body waves aided by numerical modeling of oceanic noise sources. Journal of Geophysical Research: Solid Earth, 2013, 118, 4312-4324.	3.4	43
46	Seismic Network in Greenland Monitors Earth and Ice System. Eos, 2014, 95, 13-14.	0.1	43
47	Potential Pitfalls in the Analysis and Structural Interpretation of Seismic Data from the Mars <i>InSight</i> Mission. Bulletin of the Seismological Society of America, 2021, 111, 2982-3002.	2.3	42
48	Surface wave higher-mode phase velocity measurements using a roller-coaster-type algorithm. Geophysical Journal International, 2003, 155, 289-307.	2.4	40
49	MOISE: A pilot experiment towards long term sea-floor geophysical observatories. Earth, Planets and Space, 1998, 50, 927-937.	2.5	39
50	Residual homogenization for seismic forward and inverse problems in layered media. Geophysical Journal International, 2013, 194, 470-487.	2.4	37
51	Anisotropic Tomography Around La Réunion Island From Rayleigh Waves. Journal of Geophysical Research: Solid Earth, 2017, 122, 9132-9148.	3.4	35
52	Observations of <i>S</i> 410 <i>p</i> and <i>S</i> 350 <i>p</i> phases at seismograph stations in California. Journal of Geophysical Research, 2010, 115, .	3.3	34
53	Autocorrelation of the Ground Vibrations Recorded by the SEISâ€InSight Seismometer on Mars. Journal of Geophysical Research E: Planets, 2021, 126, e2020JE006498.	3.6	34
54	The Polarization of Ambient Noise on Mars. Journal of Geophysical Research E: Planets, 2021, 126, e2020JE006545.	3.6	33

**ELEONORE STUTZMANN** 

#	Article	IF	CITATIONS
55	Anisotropic tomography of the Atlantic Ocean from Rayleigh surface waves. Physics of the Earth and Planetary Interiors, 1998, 106, 257-273.	1.9	32
56	Seismic Noise Autocorrelations on Mars. Earth and Space Science, 2021, 8, e2021EA001755.	2.6	31
57	Resonances and Lander Modes Observed by InSight on Mars (1–9ÂHz). Bulletin of the Seismological Society of America, 2021, 111, 2924-2950.	2.3	30
58	Model Space Exploration for Determining Landslide Source History from Long-Period Seismic Data. Pure and Applied Geophysics, 2015, 172, 389-413.	1.9	29
59	Large-scale flow of Indian Ocean asthenosphere driven by Réunion plume. Nature Geoscience, 2019, 12, 1043-1049.	12.9	29
60	Sea State Trends and Variability: Consistency Between Models, Altimeters, Buoys, and Seismic Data (1979–2016). Journal of Geophysical Research: Oceans, 2019, 124, 3923-3940.	2.6	29
61	The Far Side of Mars: Two Distant Marsquakes Detected by InSight. The Seismic Record, 2022, 2, 88-99.	3.1	29
62	Tomography of the transition zone from the inversion of higher-mode surface waves. Physics of the Earth and Planetary Interiors, 1994, 86, 99-115.	1.9	26
63	Lowâ€Frequency Ambient Noise Autocorrelations: Waveforms and Normal Modes. Seismological Research Letters, 2018, 89, 1488-1496.	1.9	26
64	Frequencyâ€dependent noise sources in the North Atlantic Ocean. Geochemistry, Geophysics, Geosystems, 2013, 14, 5341-5353.	2.5	25
65	Sources of secondary microseisms in the Indian Ocean. Geophysical Journal International, 2015, 202, 1180-1189.	2.4	25
66	Complex force history of a calvingâ€generated glacial earthquake derived from broadband seismic inversion. Geophysical Research Letters, 2016, 43, 1055-1065.	4.0	24
67	Joint inversion of the first overtone and fundamental mode for deep imaging at the Valhall oil field using ambient noise. Geophysical Journal International, 2018, 214, 122-132.	2.4	24
68	Poisson's ratio in the lower mantle beneath Alaska: Evidence for compositional heterogeneity. Journal of Geophysical Research, 2004, 109, .	3.3	23
69	The GEOSCOPE Program: Progress and Challenges during the Past 30 Years. Seismological Research Letters, 2010, 81, 427-452.	1.9	22
70	Towards multiscalar and multiparameter networks for the next century: The French efforts. Physics of the Earth and Planetary Interiors, 1998, 108, 155-174.	1.9	21
71	First Observation of the Earth's Permanent Free Oscillations on Ocean Bottom Seismometers. Geophysical Research Letters, 2017, 44, 10,988.	4.0	21
72	Evidence for crustal seismic anisotropy at the InSight lander site. Earth and Planetary Science Letters, 2022, 593, 117654.	4.4	21

#	Article	IF	CITATIONS
73	MOISE: A Prototype Multiparameter Ocean-Bottom Station. Bulletin of the Seismological Society of America, 2001, 91, 885-892.	2.3	20
74	Measuring Group Velocity in Seismic Noise Correlation Studies Based on Phase Coherence and Resampling Strategies. IEEE Transactions on Geoscience and Remote Sensing, 2017, 55, 1928-1935.	6.3	18
75	Tomography of crust and lithosphere in the western Indian Ocean from noise cross-correlations of land and ocean bottom seismometers. Geophysical Journal International, 2019, 219, 924-944.	2.4	18
76	Constraining landslide characteristics with Bayesian inversion of field and seismic data. Geophysical Journal International, 2020, 221, 1341-1348.	2.4	18
77	Effect of a plume on long period surface waves computed with normal modes coupling. Physics of the Earth and Planetary Interiors, 2000, 119, 57-74.	1.9	17
78	SKS splitting in the Western Indian Ocean from land and seafloor seismometers: Plume, plate and ridge signatures. Earth and Planetary Science Letters, 2018, 498, 169-184.	4.4	17
79	Monitoring Greenland ice sheet buoyancy-driven calving discharge using glacial earthquakes. Annals of Glaciology, 2019, 60, 75-95.	1.4	17
80	Constraint on the S-wave velocity at the base of the mantle. Geophysical Research Letters, 2000, 27, 1571-1574.	4.0	16
81	Global scale analysis and modelling of primary microseisms. Geophysical Journal International, 2019, 218, 560-572.	2.4	16
82	MSS/1: Singleâ€Station and Singleâ€Event Marsquake Inversion. Earth and Space Science, 2020, 7, e2020EA001118.	2.6	16
83	Towards the Processing of Large Data Volumes with Phase Crossâ€Correlation. Seismological Research Letters, 0, , .	1.9	14
84	Anatomy of Continuous Mars SEIS and Pressure Data from Unsupervised Learning. Bulletin of the Seismological Society of America, 2021, 111, 2964-2981.	2.3	14
85	The Effect of Water Column Resonance on the Spectra of Secondary Microseism <i>P</i> Waves. Journal of Geophysical Research: Solid Earth, 2017, 122, 8121-8142.	3.4	13
86	A machine-learning approach for automatic classification of volcanic seismicity at La Soufrière Volcano, Guadeloupe. Journal of Volcanology and Geothermal Research, 2021, 411, 107151.	2.1	13
87	The GEOSCOPE program: its data center. Physics of the Earth and Planetary Interiors, 1999, 113, 25-43.	1.9	12
88	The Earth's Hum Variations From a Global Model and Seismic Recordings Around the Indian Ocean. Geochemistry, Geophysics, Geosystems, 2018, 19, 4006-4020.	2.5	12
89	On PP-P differential travel time measurements. Geophysical Research Letters, 1996, 23, 1833-1836.	4.0	10
90	Quantifying microseismic noise generation from coastal reflection of gravity waves recorded by seafloor DAS. Geophysical Journal International, 2022, 231, 394-407.	2.4	10

ELEONORE STUTZMANN

#	Article	IF	CITATIONS
91	RÉSIF-SI: A Distributed Information System for French Seismological Data. Seismological Research Letters, 2021, 92, 1832-1853.	1.9	9
92	Characterization of Microseismic Noise in Cape Verde. Bulletin of the Seismological Society of America, 2019, 109, 1099-1109.	2.3	8
93	Numerical Modeling of Iceberg Capsizing Responsible for Glacial Earthquakes. Journal of Geophysical Research F: Earth Surface, 2018, 123, 3013-3033.	2.8	7
94	Mars' Background Free Oscillations. Space Science Reviews, 2019, 215, 1.	8.1	7
95	Simulation of Topography Effects on Rockfallâ€Generated Seismic Signals: Application to Piton de la Fournaise Volcano. Journal of Geophysical Research: Solid Earth, 2020, 125, e2020JB019874.	3.4	6
96	Locating Rockfalls Using Interâ€Station Ratios of Seismic Energy at Dolomieu Crater, Piton de la Fournaise Volcano. Journal of Geophysical Research F: Earth Surface, 2021, 126, e2020JF005715.	2.8	6
97	Introducing noisi: a Python tool for ambient noise cross-correlation modeling and noise source inversion. Solid Earth, 2020, 11, 1597-1615.	2.8	6
98	Imaging the crust and uppermost mantle structure of Portugal (West Iberia) with seismic ambient noise. Geophysical Journal International, 2022, 230, 1106-1120.	2.4	6
99	Preparing for InSight: Evaluation of the Blind Test for Martian Seismicity. Seismological Research Letters, 0, , .	1.9	5
100	Modelling capsizing icebergs in the open ocean. Geophysical Journal International, 2020, 223, 1265-1287.	2.4	5
101	Blind source separation of temporally independent microseisms. Geophysical Journal International, 2019, 216, 1260-1275.	2.4	4
102	Characteristic atmosphere–ocean–solid earth interactions in the Antarctic coastal and marine environment inferred from seismic and infrasound recording at Syowa Station, East Antarctica. Geological Society Special Publication, 2013, 381, 469-480.	1.3	3
103	Finding SEIS North on Mars: Comparisons Between SEIS Sundial, Inertial and Imaging Measurements and Consequences for Seismic Analysis. Earth and Space Science, 2021, 8, e2020EA001286.	2.6	3
104	Geophysical ocean bottom observatories or temporary portable networks?. Developments in Marine Technology, 2002, , 59-81.	0.5	2
105	An autonomous lunar geophysical experiment package (ALGEP) for future space missions. Experimental Astronomy, 2022, 54, 617-640.	3.7	2
106	The GEOSCOPE Program: Progress and Challenges during the Past 30 Years. Seismological Research Letters, 2013, 84, 250-250.	1.9	1
107	Seismology and Environment. Encyclopedia of Earth Sciences Series, 2020, , 1-8.	0.1	1
108	Seismology and Environment. Encyclopedia of Earth Sciences Series, 2021, , 1655-1661.	0.1	0